EVALUATING SOME COMPUTER ENHANCEMENT ALGORITHMS THAT IMPROVE THE VISIBILITY OF COMETARY MORPHOLOGY

Stephen M. Larson
Lunar and Planetary Laboratory
University of Arizona
Tucson, AZ. 85721

Charles D. Slaughter
Photometrics Ltd.
3440 Brittania Dr.
Tucson, AZ. 85706

N 9 3 - 1 9 1 9 4

ABSTRACT

Digital enhancement of cometary images is a necessary tool in studying cometary morphology. Many image processing algorithms, some developed specifically for comets, have been used to enhance the subtle, low contrast coma and tail features. We compare some of the most commonly used algorithms on two different images to evaluate their strong and weak points, and conclude that there currently exists no single "ideal" algorithm, although the radial gradient spatial filter gives the best overall result. This comparison should aid users in selecting the best algorithm to enhance particular features of interest.

INTRODUCTION

The observed morphology of cometary comae and tails is determined by ejection circumstances and the interaction of the ejected material with the cometary environment. Temporal data on the anisotropic emission of dust and gas over time can provide useful information on such things as location of active areas on the nucleus, the nucleus spin vector, and gas/dust interaction. Time sequences may also be particularly useful in following the formation and evolution of fast moving ion structures near the nucleus. However, discrete coma features are usually diffuse, of low amplitude, and they are superimposed on a steep intensity gradient radial to the nucleus. The usual 8-bit display does not usually show much detail because for large intensity ranges the contrast of coma structure is too small, or if the contrast is increased, only a small intensity range is visible.

To improve the visibility of these features, a variety of digital enhancement algorithms have been employed with varying degrees of success. They usually produced some spatial filtering, and were chosen to optimize visibility of certain detail. Since information in the image is altered, it is important to understand the effects that parameter selection and processing artifacts can have on subsequent interpretation. Our definition of the ideal algorithm is that it must enhance low contrast features while not introducing misleading artifacts. We require that features seen in the enhanced image also be seen in the unenhanced version with appropriate contrast and intensity windowing. We have not found the ideal algorithm; all of those that we have tried or developed have strong and weak elements depending upon the type of features of interest. To help assess the suitability of various algorithms, we have processed two images in a variety of ways so they can be directly compared. We attempt to identify the strong and weak points of each in the context of optimizing visibility while maintaining positional integrity of features at the expense of photometric information.

Figures 1 and 2 show the effects of various image processing on two sample images containing a variety of coma and tail features. An attempt has been made to generate hard copy that shows as

much detail as possible for each image. We do not assert that these results will be the most appropriate for other data. Experience with many data sets taken with a variety of telescopes and plate scales indicate that the sample frequency (pixel size) to resolution ratio can be important in selecting the algorithm or processing parameters. In general, there is more parameter leeway with over-sampled data (pixel size/"resolution"< 1) than for under-sampled data because of reduced centroid (or registration) uncertainty and pixelization artifacts are smaller relative to the features of interest. The two sample images and their processed versions are shown in Figures 1 A-H and 2 A-H. The figure letters correspond to the subheading letters below.

A. THE UNPROCESSED IMAGES

The sample image in Figure 1 is a composite which includes a mostly H_2O^+ CCD image of P/ Brorsen-Metcalf taken with a narrow-band filter transmitting the H_2O^+ (0,8,0) band near 619 nm, and some of the C_2 (0,2) band. This comet was extremely dust-poor, so the ion streamers were relatively high contrast, and the C_2 is easily seen to be restricted near the nucleus. However, since this is not usually the case for a "typical" dusty comet, we have added a 1/r intensity gradient to the central condensation that might be expected from isotropic emission of dust from a rapidly rotating nucleus. The resulting test image has a "dust"/ion intensity ratio of 50:1. A second combination using an image of P/Brorsen-Metcalf taken 15 minutes later was used for the temporal derivative. The scale of the image is 0.7 arcsec per pixel, or 400 km per pixel at the comet.

The sample image in Figure 2 is a broad red-band CCD image of P/Halley that contains several dust jets, an antisunward dust jet, and ion streamers. A second image taken 45 minutes later was used for the temporal derivative. Both are three co-added 120 second exposures, and are also 0.7 arcsec per pixel, or 640 km per pixel at the comet.

B. LOG 10 INTENSITIES

The simplest operation is to alter the intensity scale by some non-linear contrast stretch (such as the base 10 logarithm) to suppresses the steep intensity peak near the photocenter. In this case, the resulting pixel value (I) becomes;

$$I_{(x, y)} = \log I_{o(x, y)}$$

where I_0 = original pixel count value. This helps bring the brightness of the faint outer regions of the coma closer to those in the inner coma. No artifacts are introduced, but there is only a modest improvement in visibility of low contrast features. In general, such non-linear stretches do not allow appreciable increase in local feature contrast relative to the background. The subjective result is to convert linear-response electronic images to a photographic-like response. The strong point is that the image is easily understandable and interpretation is straight forward. Because the operation involves no special parameter selection (or "interpretation"), this is the form Near Nucleus Studies Network images appear in the International Halley Watch printed archive.

SPATIAL DERIVATIVES

C. Linear Shift-difference

Spatial derivative, or "shift-difference" algorithms enhance intensity discontinuities, but only in the direction of the shift (Klinglesmith, 1982);

$$I_{(x, y)} = I_{o(x, y)} - I_{o(x+n, y+m)}$$

where, n, m are the amount of the shift in x and y. The simple linear shift-difference is very effective for bringing out ion tail structure when the shift is perpendicular to the tail axis. The magnitude of shift is a compromise between showing the smallest detail and enhancing the noise. The most serious problems with this method is that the results are directionally dependent, and are

not easily interpretable. The resulting features, showing the rate of change of intensity, enhance the edges of jets and shells. In both of these examples, the shift is perpendicular to the tail axis to best show the ion features. The residual radial gradient is directly related to the magnitude of shift. However, a smaller shift would leave only the highest spatial frequencies (mostly system noise). Coma detail is particularly difficult to interpret.

D. Rotational Shift-difference

Radial and rotational shift-difference algorithms were developed in response to the fact that particles generally move radially away from the nucleus, and that nucleus rotation produces spiral features (Larson and Sekanina, 1984). In polar coordinates, the combination radial and rotational shift gives;

$$I_{(r,\theta)} = I_{0(r,\theta)} - I_{((r+\Delta r), (\theta+\Delta\theta))}$$

where Δr = the radial shift, and $\Delta\theta$ = the rotational shift. The rotational derivative used in this comparison emphasizes rotational intensity discontinuities, such as radial jets and ion streamers. A radial derivative emphasizes discontinuities concentric to the nucleus, such as hoods and evolved jets. In one variation, such shifts are done in combination with rotational shifts of different directions but different amounts to reduce the directional dependency of the enhancement. The reproduced images show features in a 10^0 rotational derivative, however, ion streamer overlap may cause confusing aliasing. The angular shift produces a radial dependency on the linear scale of edges that become enhanced. For some types of gas jets that become more diffuse farther from the nucleus, rotational shift-differencing is useful, but for ion features, it is usually confusing. With the rotational derivative, it is possible to see features down to the central condensation.

Since the synthetic test image contains no radial discontinuities, nothing appears in a radial shift-difference, but the Comet Halley image shows the outer envelope well. By combining the radial plus rotational shift difference the directional dependency of feature visibility is reduced but not eliminated. Interpretation requires great care since it is the edges of features that are enhanced. Finding the best combination of rotational and radial shifts can be difficult and enhances only a limited spatial frequency range. Radial and combination derivatives are not shown in the figures.

E. TEMPORAL DERIVATIVE

Differencing carefully registered images taken at different times yield features that have moved. Such temporal derivative images are projected velocity maps that (among other things) make it easy to distinguish rapidly varying ion features from the slower moving dust structures (e.g. Larson and Minton, 1971; Larson, 1986).

$$I_{(x, y)} = I_{0(xt_1, yt_1)} - I_{0(xt_2, yt_2)}$$

where t_1 and t_2 are different times. Successful short-term difference images bring out ion features which are normally a minor component of a broad-band image. This method places great demands upon sets of images with nearly identical quality and very precise registration. Registration on the centroid of a several pixel area around the central condensation is usually necessary to reduce the effects of noise. Variations in seeing and guiding can complicate the result. Interpretation must be made with care, since the result is an image of moving feature edges.

The synthetic test image processed this way shows the ion features best of all of the algorithms used, as all of the radial intensity gradient is eliminated. The rapid ion motions require images taken only a few minutes apart to show detail at this resolution. The Comet Halley image also shows the ion streamer motions, but also a lot of garbage resulting from imperfect flat fields, scattered twilight, and possible differential extinction at the large airmass. These problems cause the coma to have dark and light components that have nothing to do with the comet. The best temporal derivatives resulting from consistent, regularly spaced sequences of images are relatively easy to interpret.

F. AZIMUTHAL RENORMALIZATION

Azimuthal function algorithms reduce the radial gradient by either subtracting the average value in the annulus of constant distance from the photocenter, or by subtracting a best-fit, low- order function to the annulus (A'Hearn, et al., 1986).

$$I(r, \theta) = Io(r, \theta) - ((\Sigma\, I(r))/n))$$

where n = number of pixels falling within the annulus of radius r, and are summed over all theta. Averaging and function fitting is more easily done after a polar to rectangular coordinate transformation (with the photocenter at the origin). This method is very efficient in eliminating the radial gradient, does not have any directional dependencies, and interpretation is straight-forward. The photocenter must be determined very carefully, especially for undersampled data, or spurious features close to the nucleus may be produced. Options in the A'Hearn and Klavetter (Univ. Maryland) program includes normalization to mean or median values at constant radius, or normalizing to a functional profile. Our own implementation of this algorithm normalizes to the mean of the annulus without a polar to rectangular coordinate conversion step (fig. 2F).

The synthetic image responds very well by eliminating all of the radial gradient and leaving the ion features intact. The noise becomes rather apparent, but there are options for averaging over various ranges of r and theta that the authors did not have time to try. We are not confident that the optimum parameters for this algorithm were used, however, the result is the most easily interpretable version for this image. The Comet Halley image, primarily because of the large amplitude of the sunward asymmetry, does not respond as well to an azimuthal normalization to a mean value. Similarly, normalization to an azimuthally symmetric function produces over-compensation in the tail direction, and under-compensation in the sunward direction. Although this algorithm does not work very well for primarily continuum images it works very well on images of the more symmetrical gas comets.

Another approach is to subtract a synthetic image based on a generalized model of particle outflow. This assumes some *a priori* knowledge of the ejection function. If there is enough data, subtraction of a mask produced by the median of many images over time may also work (Jewitt, 1991). In a sense, this is similar to a temporal derivative.

G. SPATIAL FILTERING

Traditional spatial filtering algorithms reduce the radial gradient by eliminating the low spatial frequency domain in the image. A "high-pass" gaussian deconvolution retains features in the image smaller than the gaussian, and by eliminating the broad radial gradient, the contrast of the smaller features can be increased. There is no directional dependency, but "ringing" artifacts can be seen around bright stars and the central condensation of the comet. Selecting the optimum size gaussian usually depends upon the characteristic size of the features of interest. Although large, complete filter kernels are more rigorous, our spatial filtering algorithm uses an abbreviated kernel convolution to reduce the computation time. A 3 x 3 pixel kernel is used, but the kernel size is adjusted by varying the spacing between kernel pixels. This allows filtering over a wide range of spatial domains, while operating on a small number of pixels. The kernel shape is dictated by weights given the "corner" and "medial" pixels in the kernel.

$$I_{(r, \theta)} = I_{o(r,\theta)} - \Sigma I_{o(r',\theta')}w_1 - \Sigma I_{o(r'',\theta'')}w_2$$

where; w_1 = "corner" weights; w_2 = "medial" weights, nominally $(w_1 + w_2) = 1.0$;
$\Delta x = \Delta y$ = kernel pixel separation, and $r = (x^2 + y^2)^{1/2}$, $r' = ((x \pm \Delta x)^2 + (y \mp \Delta y)^2)^{1/2}$;
$r'' = (x^2 + (y \mp \Delta y)^2)^{1/2}$; $((x \pm \Delta x)^2 + y^2)^{1/2}$, θ = arctan (y/x); θ' = arctan $((y \mp \Delta y)/(x \pm \Delta x))$,
θ'' = arctan (y/(x \pm \Delta x)), $((y \mp \Delta y)/x)$

Processing the synthetic image brings out the ion tail fairly well up to the point that the spatial component of the radial gradient becomes smaller than the effective kernel FWHM near the

central condensation. Use of a smaller kernel to reduce this residual gradient emphasizes the noise and is better suited to high S/N ratio images. The P/Halley image shows nearly all of the jet, envelope and ion features quite well. The kernel size was chosen to optimize over-all visibility of features, but there is a residual small gradient close to the central condensation. Interpretation of this image is not difficult.

H. RADIAL GRADIENT SPATIAL FILTERING

Since cometary features typically become larger farther from the nucleus, spatially selective spatial filtering might be desirable. We have recently developed a variable kernel deconvolution routine that passes increasingly higher frequencies closer to the photocenter. This enhances a larger spatial range of coma features which often exist in an image. The previous algorithm is used, but the spacing $(\Delta x, \Delta y)$ is variable from the photocenter;

$$\Delta x = \Delta y = (a + (r/b)), a = \text{kernel pixel separation}, b = \text{radial scale factor.}$$

The processed synthetic image shows the ion tail well, but does not show the folding rays as well as the temporal derivative. Note the strong pixelization pattern radiating from the nucleus. The processed P/Halley image shows detail of the central condensation as well as the ion streamers. The parameters w_1, w_2, a and b must be chosen empirically to ensure that features in the various spatial regimes are visible. Field stars may present problems with "ringing" (dot patterns in this abbreviated kernel).

CONCLUSIONS

We find that for coma jets, spatial filtering provides the best overall enhancement with minimal artifacts, and the results are readily interpretable. The radially variable convolution kernel provides a range of spatial filtering appropriate for different regions of the comet (high-pass at the center, lower near the edges). For ion structure, we find that temporal derivatives are the most useful in not only bringing out low contrast detail, but providing a "velocity map" of ion motions.

Acknowledgments

References

A'Hearn, M. F., Hoban, S., Birch, P.V., Bowers, C., Martin, R., and Klinglesmith, D.A. (1986) Cyanogen jets in Comet Halley, Nature, 324, 649-651.

Jewitt, D. (1991) Cometary photometry. In Comets in the Post-Halley Era (R. L. Newburn, M. Neugebauer and J. Rahe eds.), pp 19-65. Kluwer, Dordrecht.

Klinglesmith, D. A. (1981) The interactive astronomical data analysis facility - - Image enhancement techniques applied to Comet Halley. In Modern Observational Techniques for Comets (J. C. Brandt, J. M. Greenberg, B. Donn and J. Rahe eds.) pp. 223-231. JPL publication 81-68, Pasadena.

Larson, S. M.(1986) A review of some digital image processing in cometary research. In Asteroids Comets Meteors II (C. -I. Lagerkvist, B. A. Lindblad, H. Lundstedt, and H. Rickman, eds.), pp. 449-459. Uppsala universitet, Uppsala.

Larson, S. M. and Minton, R. B. (1972) Photographic observations of Comet Bennet, 1970II. In Comets - Scientific Data and Missions (G. P. Kuiper and E. Roemer, eds.), pp. 183-208. Lunar and Planetary Laboratory, Tucson.

Larson, S. M. and Sekanina, Z. (1984) Coma morphology and dust emission pattern of periodic Comet Halley.I. High resolution images taken at Mount Wilson in 1910. Astron. J., 89, No.4, 571-578 and 600-606.
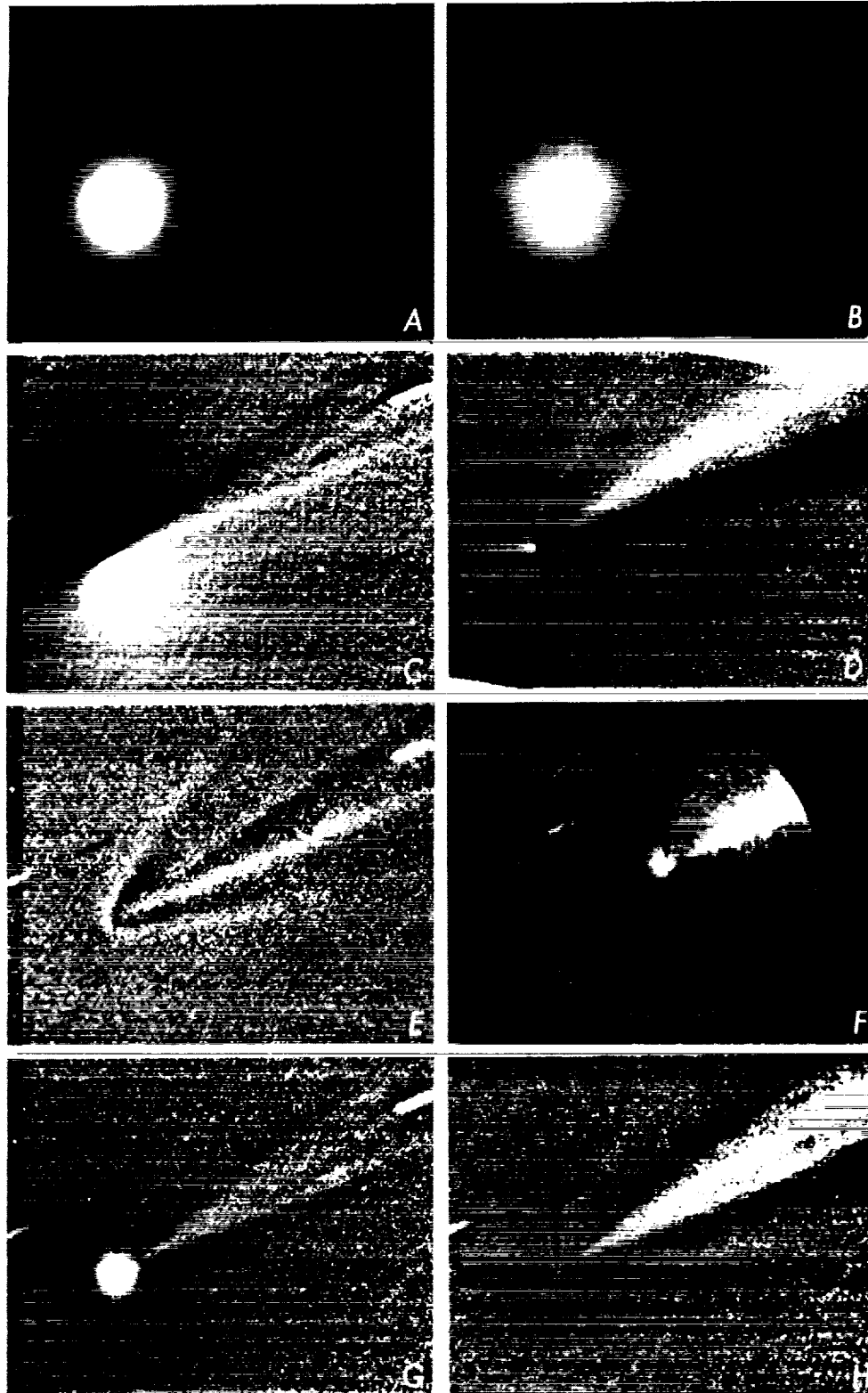
Fig. 1. A. Test image with ion features and a symmetric 1/r intensity gradient (see text), B. displayed as the base 10 logarithm of the counts, C.linear derivative (perpendicular to the tail axis), D. rotational derivative, E. temporal derivative, F. azimuthal renormalization, G. constant spatial filter, and H. radially varying spatial filter.
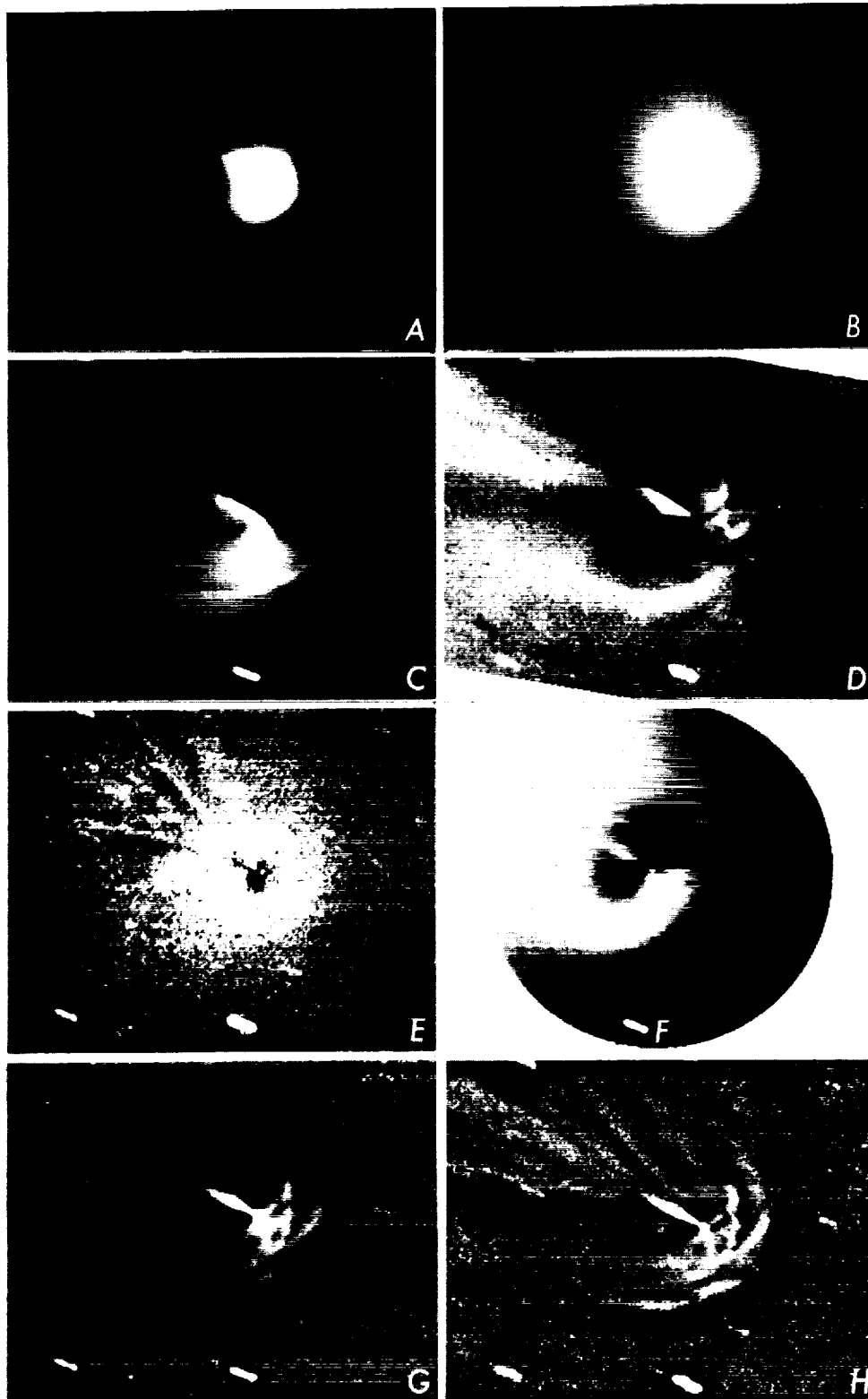
Fig. 2 A. Image of P/Halley (see text), B. displayed as the base 10 logarithm of the counts, C. linear derivative (perpendicular to the tail axis), D. rotational derivative, E. temporal derivative, F. azimuthal renormalization, G. constant spatial filter, and H. radially varying spatial filter.